Probing pH and Pressure Effects on the Apomyoglobin Heme Pocket with the 2′-(*N*,*N*-dimethylamino)-6-naphthoyl-4-*trans*-cyclohexanoic Acid Fluorophore

Olivier Sire,* Bernard Alpert,* and Catherine A. Royer‡
*Laboratoire de Biologie Physico-Chimique, Université—Paris 7, Denis Diderot, 75251 Paris, France; and ‡School of Pharmacy, University of Wisconsin, Madison Wisconsin 53706 USA

ABSTRACT The environmentally sensitive fluorophore 2′-(*N*,*N*-dimethylamino)-6-naphthoyl-4-*trans*-cyclohexanoic acid (DANCA) has been used to probe the apomyoglobin heme pocket. The unexpected polarity of this domain is generally interpreted as arising from dynamic dipolar relaxation of the peptide dipoles surrounding the heme pocket. In the present work we reexamine the photophysical properties of DANCA in a variety of solvents and complexed with apomyoglobin (apoMb) to further probe the heme pocket environment as a function of external solvent conditions. Absorption and excitation spectra in a number of solvents are consistent with the well-known $\pi^* \leftarrow \pi$ (LE) and $\pi^* \leftarrow n$ (CT) electronic absorption transitions observed for naphthylamine derivatives. Dual emission is also a well-documented property of such derivatives. Based on the time scale of the heterogeneity in the decay of the DANCA fluorophore observed in a series of solvents, we propose that the emission properties of DANCA in apoMb are not uniquely attributable to dynamic relaxation events, but also reflect dual emission from both a long-lived, red CT state and the shorter-lived, blue LE state. The pH studies in the range of pH 5–9 of the emission properties of DANCA in apoMb support this hypothesis. They also suggest a specific interaction of DANCA with one or both of the pocket histidyl residues, which leads to a drastic static quenching and red shift of the bound DANCA fluorescence upon protonation. Similar effects are observed with increasing pressure, indicating that these two perturbations alter the DANCA-apoMb complex in a similar fashion. The pressure-induced form of the protein is distinct both energetically and structurally from the previously characterized acid intermediate, in that it is populated above pH 5 and retains a significant degree of integrity of the heme pocket.

INTRODUCTION

2′-(*N*-*N*-dimethyl) amino-6-naphthoyl-4-*trans*-cyclo-hexanoic-acid (DANCA), which binds the apomyoglobin heme pocket (apoMb), has been used to probe its polarity and dynamics (MacGregor and Weber, 1986; Pierce and Boxer, 1992). These previous fluorescence studies demonstrated that the environment of the heme pocket is less hydrophobic in character than was generally acknowledged, because, though it is lined with nonpolar amino acids (Kendrew, 1960), DANCA emission energy indicates a polarity similar to that of dimethylformamide (DMF). This unexpected polarity was interpreted as arising from dynamic relaxation of the surrounding peptide dipoles. The time-resolved properties of DANCA (Pierce and Boxer, 1992) and similar derivatives (Gafni et al., 1977, Lakowicz et al., 1984; Bashkin et al., 1990) complexed with apoMb have been analyzed in terms of dynamic relaxation of the surrounding peptide dipoles leading to a single, time-dependent emission spectrum.

In the present studies, we have investigated the absorption, excitation, steady-state, and time-resolved fluorescence properties of DANCA in a series of solvents and in the heme pocket of horse heart apoMb. Moreover, the pH and pressure dependence of the fluorescence properties of the apoMb-DANCA complex have been investigated as a means of determining the effects of these variables on the heme pocket environment.

Received for publication 5 July 1995 and in final form 7 February 1996.
Address reprint requests to Dr. Catherine A. Royer, University of Wisconsin, School of Pharmacy, 425 N. Charter Street, Madison, WI 53706. Tel.: 608-262-7810; Fax: 608-262-3397; E-mail: car@pharmacy.wisc.edu.

0006-3495/96/06/2903/12 $2.00

MATERIALS AND METHODS

Sample preparation

DANCA was generously provided by Professor Gregorio Weber from the University of Illinois. Equal amounts of desiccated DANCA powder were dissolved in the various solvents studied. All solvents were spectroscopic grade from Aldrich, Milwaukee, WI. Except in cyclohexane, DANCA solubility was sufficient for collecting absorption spectra, though DANCA was not fully solvated in benzene. The concentration of DANCA was determined spectrophotometrically from the water sample (50 mM bis Tris pH 6.25) using ϵ = 14,000 cm^2 M^{-1} at 360 nm (MacGregor and Weber, 1986).

Horse heart myoglobin was obtained from Sigma (St. Louis, MO) and was used without further purification. apoMb was prepared according to the Teale method (Teale, 1959). The apoprotein stock solution was then lyophylized. The apoMb and DANCA concentrations in the solution samples were determined optically at 280 nm (ϵ = 13,500 M^{-1} cm^{-1}) and 360 nm (ϵ = 14,000 M^{-1} cm^{-1}), respectively. Samples were buffered with 50 mM bis-Tris or Tris salt. These buffers were chosen because their dissociation constants do not vary with pressure (Neuman et al., 1973). pHs were adjusted using standard solutions equilibrated at the same temperature as used in the experiments. The protein samples were allowed to equilibrate overnight and pH values were corrected if necessary.

Absorption and steady-state fluorescence measurements

All absorption and fluorescence experiments were carried out at 20°C in a thermostated cell holder with ~1°C accuracy. Absorption spectra were recorded on an updated Cary 14 spectrophotometer (On-line Instrument Systems, Inc., Bogart, GA) with a 1-nm slit. These spectra were best fit in wavenumber space by two Gaussian components, termed A1 and A2. Steady-state fluorescence emission spectra were acquired with an excitation wavelength of 350 nm and a 8-nm band pass in both excitation and emission. All spectra were corrected for grating transmission and detector response before further treatment. Measurements were performed on an ISS KOALA (ISS, Urbana, IL). The emission mass center ν_g, was calculated using the ISS spectral software as

$$\nu_g = \sum_i F_i \nu_i / \sum_i F_i \quad (1)$$

were ν_i is the emission energy in wavenumbers and F_i is the corresponding intensity at that energy. Emission spectra in wavenumber space were best fit to four symmetric Gaussian components using nonlinear least-squares regression. The average confidence limits for each fitted parameter (position, intensity, and halfwidth for each band) were estimated from the χ^2 probability function ($p < 0.67$). Typical confidence intervals were 10 cm^{-1} (0.2 nm) (position), 1.5% (intensity) and 15 cm^{-1} (0.5 nm) (halfwidth).

Time-resolved fluorescence measurements

The fluorescence lifetimes of DANCA in three different solvents and in apoMb were determined by multifrequency fluorometry on an ISS analog fluorometer using the harmonic content of a mode-locked laser. The excitation light at 355 nm was provided by the mode-locked frequency-doubled output of an Antares Nd-YAG laser (all components from Coherent Corp., Palo Alto, CA). The output was then frequency tripled with a Coherent Third Harmonic generator (λ_{exc} = 355 nm) and pulse picked at 3.785 MHz using an external Bragg cell (NEOS, Melbourne, FL) driven with the Coherent cavity dumping electronics. The frequency responses of the phase and modulation of the fluorescence are referenced hereafter as frequency response curves. Frequency response curves were collected at 390, 410, 430, 450, and 470 nm in TEA; at 440, 460, 480, 500, and 520 nm in ethanol; at 494, 510, 522, 530, 550, and 570 nm in water. In apoMb frequency response curves were collected from 400 to 480 nm in 10-nm wavelength intervals. Thus, only the emission corresponding to the bound DANCA was observed because the weak emission from the very small amounts of free DANCA occurs at longer wavelengths (from 480 to 600 nm).

The fluorescence intensity decay was expressed as:

$$I(t) = \sum_i \alpha_i e^{-t/\tau_i} \quad (2)$$

where $\alpha_{i,\lambda}$ is the pre-exponential concentration factor and τ_i is the lifetime for the ith emitting component. The fractional contribution to the total fluorescence intensity, f_i, for the ith emitting component is related to its corresponding pre-exponential factor as follows:

$$fi = (\alpha_i \tau_i) / \sum_i \alpha_i \tau_i \quad (3)$$

The frequency response of the fluorophore is the Fourier transform of the intensity decay function, $I(t)$, where G and S are the real and imaginary parts of the transform, respectively:

$$G = \int_0^\infty I(t) \cos \omega t \, dt \quad (4)$$

$$S = \int_0^\infty I(t) \sin \omega t \, dt \quad (5)$$

The phase angle, ϕ, relative to excitation and the modulation ratio, M, measured at frequency ω, are related to the sine and cosine Fourier transforms of the fluorescence decay function, S and G, as follows:

$$\tan \phi = -\omega\tau \quad (6)$$

$$M = (S^2 + G^2)/I_{tot} \quad (7)$$

Multi-wavelength data sets were analyzed for linked lifetime and unlinked fractional intensities to yield decay associated spectra (DAS) with the global analysis software Globals Unlimited (LFD, Urbana, IL), which is described in detail elsewhere (Beechem et al., 1992). Average lifetimes were fractional intensity rather than fractional population weighted for direct comparison with intensity profiles.

For the generation of time-resolved emission spectra (TRES) from the results of the DAS analysis, the analysis was carried out in terms of amplitudes rather than fractional intensities, and the time-domain decay curves with appropriate weighting were simulated using the product of the recovered fractional amplitude values from the multi-exponential fits and the total intensity values at each wavelength as the pre-exponential factors.

$$I_{(t,\lambda)} = \sum \alpha_{(i,\lambda)} I_{(\lambda)} e^{-t/\tau i} \quad (8)$$

The TRES were constructed from the absolute values of the emission intensities at the tested wavelengths at various time intervals. The evolution of these spectra with time was represented as the time-dependence of the average emission energy ν_g of the simulated TRES as per Eq. 1. Analysis in terms of excited-state electron transfer was carried out using the eigenvector-eigenvalue numerically based compartmental analysis routines in the global analysis software as described by Beechem et al. (1992).

Fluorescence anisotropy measurements

We used DANCA fluorescence anisotropy to evaluate the affinity of horse apoMb for DANCA. For identical DANCA concentrations, the emission intensity of bound DANCA is approximately four times as intense at the maximal emission wavelength as the emission of the free DANCA. Upon apoMb binding, DANCA emission is also considerably blue shifted (~80 nm) as compared with free DANCA in water (MacGregor and Weber, 1986). Titrations involving sequential additions of apomyoglobin were carried out at 20°C in the presence of 1 μM DANCA, by monitoring the fluorescence anisotropy at 480 nm. Anisotropy data were fit for the binding constant with the BIOEQS program (Royer et al., 1992; Royer and Beechem, 1992; Royer, 1993) using the appropriate fourfold quantum yield factor to account for the increase in fluorescence yield between free and apoMb-bound DANCA. Analysis of fluorescence anisotropy curves obtained in bis-Tris, 20°C, pH 6.20 yielded a K_d value that is twice as large as the value reported for sperm whale apoMb (MacGregor and Weber, 1986) for which the quantum yield correction was not made. Hence, emission spectra of the apoMb-DANCA complex were typically collected at protein and DANCA concentrations (0.4 mM and 5 μM, respectively) such that 98% of the total emission intensity arises from the bound form corresponding to a 0.94 bound fraction.

Pressure experiments

Pressure experiments were carried out in a Vascomax 300 (Teledyne Vasco, Elk Grove, IL) thermostated pressure bomb equipped with four quartz windows rated to 2.5 kbar. Emission spectra were recorded for various pH values from 1 atm to 2.5 kbar with 0.3-kbar pressure intervals. The emission spectra were recorded 10 min after each pressure increase to allow the signal to stabilize. The pressure effect on the DANCA lifetimes was investigated at pH 6.2. To assess whether the observed pressure effects on the DANCA emission spectrum were related to pressure-induced DANCA dissociation from the heme pocket, fluorescence anisotropy measurements were conducted. For this purpose, a special cell holder, equipped with 3 film polarizers (Omega Optics, Battleboro, VT) vertical in excita-

tion and two crossed polarizers (one vertical and one horizontal) in the two emission channels at 90° to excitation, was designed to fit the inner chamber of the pressure cell. In this case, anisotropy measurements were performed in T-format, which allows a simultaneous recording of vertical and horizontal polarized intensities. This cell was calibrated with a Ficoll suspension as a source of light scattering and a 1-diethylamino naphthalene-8-sulfonate (DENS) solution, which exhibits sufficiently long fluorescence lifetime ($\tau \sim 30$ ns) to yield an almost completely depolarized signal. This allows the estimation of pressure-dependent g-factor to be applied as pressure is increased. The total intensity and the average emission energy of the DANCA fluorophore as a function of pressure were fit to a model of a single protein conformational change with an associated free energy and a volume change for the transition using the BIOEQS program described previously (Royer et al., 1992; Royer and Beechem, 1992; Royer, 1993). The emission energy was quantum yield weighted for the loss in intensity observed as a function of pressure.

RESULTS AND DISCUSSION

The absorption maxima of DANCA in a series of solvents and in the heme pocket of horse heart apoMb at pH 7.5, as well as the optical density ratio with respect to DANCA in water are given in Table 1. The absorption spectrum of DANCA in triethylamine (TEA), DMF, apoMb, ethanol, and water, respectively in Figs. 1 *a–e*, can be seen to be quite sensitive to the solvent both in the absorption maximum and the spectral bandwidth. At least two absorption peaks are apparent in these spectra, and the lower energy transition is much less evident in the apolar TEA than in the other solvents or the heme pocket. These DANCA absorption spectra were best fit by two symmetric Gaussian bands, referred to here as A1 and A2. In TEA the highest energy absorption band (A1) predominates; as the polarity of the solvent increases from DMF to ethanol to water, the lower energy component contributes progressively more to the absorption spectrum, and its maximum shifts significantly to lower energy. The absorption maxima for the two Gaussian bands and the fractional contributions to the absorption of the two bands are given in Table 2.

The excitation spectrum of DANCA in Tris buffer at pH 7 provides further information concerning the heterogeneity of its absorption transitions (Fig. 1 *f*). It is clear from examination of this spectrum that at least three spectral components are present. In fact, it was best fit to four symmetric Gaussian bands. The peak of the low energy transition (A2) obtained from the two-component fits of the absorption spectrum in water (393 nm) agrees well with the peak maximum of component three in the excitation spectrum (391 nm). The high energy A1 peak at 350 nm in absorption is quite broad, and in the excitation spectrum there are clearly two components in this wavelength range with maxima respectively at 343 and 370 nm. We note that the choice of symmetric Gaussian functions for fitting the spectral envelopes is somewhat arbitrary, and the existence of the fourth component, as well as the exact shape of the underlying other spectral components may well be influenced by this choice of fitting function. Nonetheless, there are clearly at least three electronic absorption transitions for DANCA in the wavelength range monitored.

Methylamine derivatives of conjugated ring systems are well known to exhibit an $\pi^* \leftarrow n$ charge transfer band (CT), as well as the typical aromatic ^1L_a and ^1L_b and B type $\pi^* \leftarrow \pi$ absorption transitions (Suzuki, 1967, Grabowski et al., 1979; Kosower, 1985; Kosower and Huppert, 1986; Ilich and Prendergast, 1989). The CT bands involve partial electron transfer from the somewhat planar amino group (Suzuki, 1967) to the conjugated ring system, rotation of the amino group (Grabowski et al., 1979), and some ring distortion (Ilich and Prendergast, 1989). The oscillator

TABLE 1 Spectral properties of DANCA solutions

Solvent	Absorption, max (nm)	Emission max (nm)	OD ratio	Q.Y. ratio	Δf
Cyclohexane	nd	391	nd	nd	0.001
Benzene	352	417	nd	nd	0.002
TEA	346	399	1.56	0.37	0.102
Cl-benzene	363	425	1.07	1.22	0.143
Chloroform	372	435	0.87	5.78	0.185
Acetone	354	441	1.93	5.18	0.287
DMF	357	448	2.08	5.00	0.287
apoMb*	364	446	—	4.00	—
Acetonitrile	357	451	1.15	3.28	0.276
Et-glycol	392	495	1.77	2.68	0.304
Ethanol	368	479	1.87	4.27	0.274
Methanol	371	489	1.82	3.63	0.298
Water	367	519	1	1	0.320

The OD ratio is defined by the OD in the corresponding solvent normalized to that in water at the same concentration. The quantum yield ratio corresponds similarly to the integrated emission area normalized for an OD at the excitation wavelength (350 nm) of 0.07, relative to that in water. (OD is measured at 350 nm). nd = nondetermined.

Δf refers to the orientational polarizability defined as

$$\Delta f = [(D - 1)/(2D + 1)] - [(n^2 - 1)/(2n^2 + 1)],$$

where D is the dielectric constant and n is the refractive index.

*ThesedatawerecollectedatpH7.0.

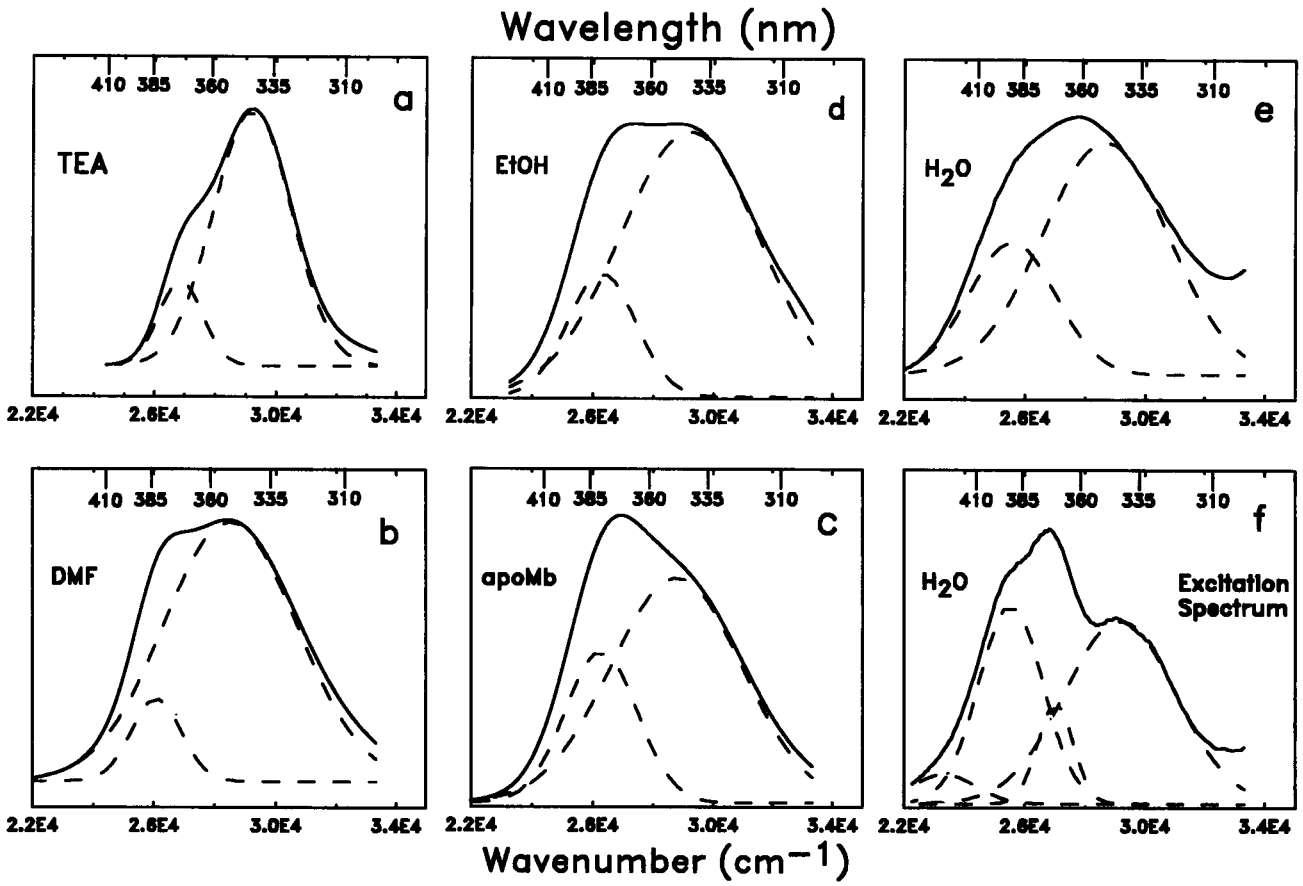

FIGURE 1 Absorption spectra of DANCA in *a*) TEA, *b*) DMF, *c*) apomyoglobin, *d*) ethanol, and *e*) water; and *f*) excitation spectrum of DANCA in water. Absorption spectra have been fitted to two and excitation spectra to four symmetric Gaussian bands as described in Materials and Methods. Spectra were collected at 20°C.

strengths of the CT transitions are particularly strong in the case of para-substitutions of electron accepting groups (Suzuki, 1967), as is the case for the carbonyl in the 6 position of DANCA. In fact, this strong absorption and the CT character of these transitions is what inspired the synthesis of 6-proprionyl-2(dimethylamino)naphthalene (PRODAN), a precursor of DANCA (Weber and Farris, 1976). The solvent dependence of the position and oscillator strength of the A2 absorption band supports its assignment as the CT band. In fact, in TEA, the wavelength maximum for the CT absorption transition (391 nm) is very close to that obtained from molecular orbital calculations (388 nm) (Illich and Prendergast, 1989). The other two transitions may well correspond to the ^1L_a and ^1L_b bands, which these authors previously calculated to be at 355 and 365 nm, respectively, while noting that their assignment had yet to be made. We have measured the excitation dependence of the polarization of fluorescence of DANCA in glycerol at −50°C. The excitaiton polarization spectrum exhibits low values below 320 nm, corresponding the the edge of the B-band $\pi^* \leftarrow \pi$ transition. There is a small increase from 320 to 420 nm, indicative of more than one transition over this range.

TABLE 2 Wavelength maxima and relative contribution at 350 nm of the two DANCA absorption components

Solvent	A1	%A1	A2	%A2
TEA	343.2 (nm) 29140 (cm^{-1})	99	373.4 (nm) 26830 (cm^{-1})	1
DMF	350.9 (nm) 28500 (cm^{-1})	87.4	383.6 (nm) 26070 (cm^{-1})	12.6
apoMb*	347.5 (nm) 28780 (cm^{-1})	69.6	380.5 (nm) 26280 (cm^{-1})	30.5
Ethanol	342.11 (nm) 29230 (cm^{-1})	94	380.81 (nm) 26260 (cm^{-1})	6
Water	352.11 (nm) 28400 (cm^{-1})	97	393.86 (nm) 25390 (cm^{-1})	3

*These data were collected at pH 7.0.

The emission spectrum of DANCA in TEA, DMF, apoMb (pH 7.5), ethanol, and water is seen in Fig. 2 *a–e* to shift red with increasing solvent polarity. The solvent dependence of the emission of DANCA is summarized in Table 1. The spectrum of DANCA in apoMb most closely resembles that in DMF as noted previously (MacGregor and Weber, 1986). The spectra in all solvents are well described by four symmetric Gaussian components whose relative contribution to the emission spectrum is sharply dependent upon the nature of the solvent. These four Gaussian com-

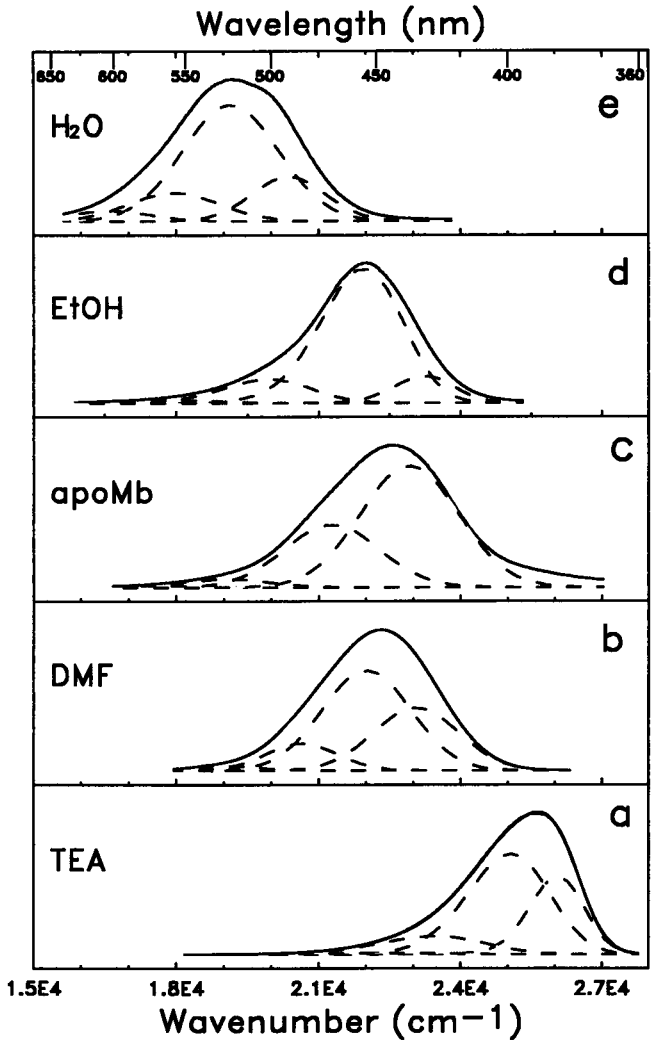

FIGURE 2 Corrected fluorescence emission spectra at 20°C of DANCA in *a*) TEA, *b*) DMF, *c*) apomyoglobin, *d*) ethanol, and *e*) water excited at 350 nm, 20°C. Spectra are normalized to the full scale of the graph and do not represent relative intensities between the different solvent systems. The figure also displays (*dash lines*) the four symmetric Gaussian components obtained by the nonlinear fitting of the data.

ponents of the DANCA spectra are referred to as C1–C4, moving from high to low energy. The bluest component, C1, appears to contribute most significantly to the total emission in apolar solvents such as TEA and in the heme pocket of apoMb. It is less evident in DMF and contributes little in ethanol and water.

Although fitting of the spectral envelopes by symmetric Gaussian bands is somewhat arbitrary, the differences in the symmetries of DANCA emission spectra in these solvents indicated that there was nonetheless an underlying heterogeneity to the emission spectrum. If the spectral components from the Gaussian fits are indeed a reflection of heterogeneous emission from DANCA, then such heterogeneity should be evident in the time-resolved emission properties as well. Although it is true that dynamic solvent relaxation contributes to the apparent heterogeneity of the fluorescence decay, at room temperature in low viscosity neat solvents such as TEA, ethanol, and water, the time scales for either longitudinal or dielectric relaxation are quite fast, femtoseconds to picoseconds (Maroncelli and Fleming, 1985; Fleming, 1986), and with the time-resolution of our equipment (> 50 ps), such relaxation phenomena should not be observed. The frequency response curves at five emission wavelengths for DANCA in TEA, ethanol, and water are shown in Fig. 3. All solvents exhibit wavelength heterogeneity, although this is most evident in TEA. Phase and modulation curves generally shift to lower frequencies with increasing wavelength, indicative of a longer-lived fluorescence on the red edge.

We first analyzed the frequency response curves in these solvents in terms of two or three time-invariant decay associated spectra (DAS), as shown in Fig. 4. In TEA, the most prominent recovered component exhibits a 0.3-ns life-

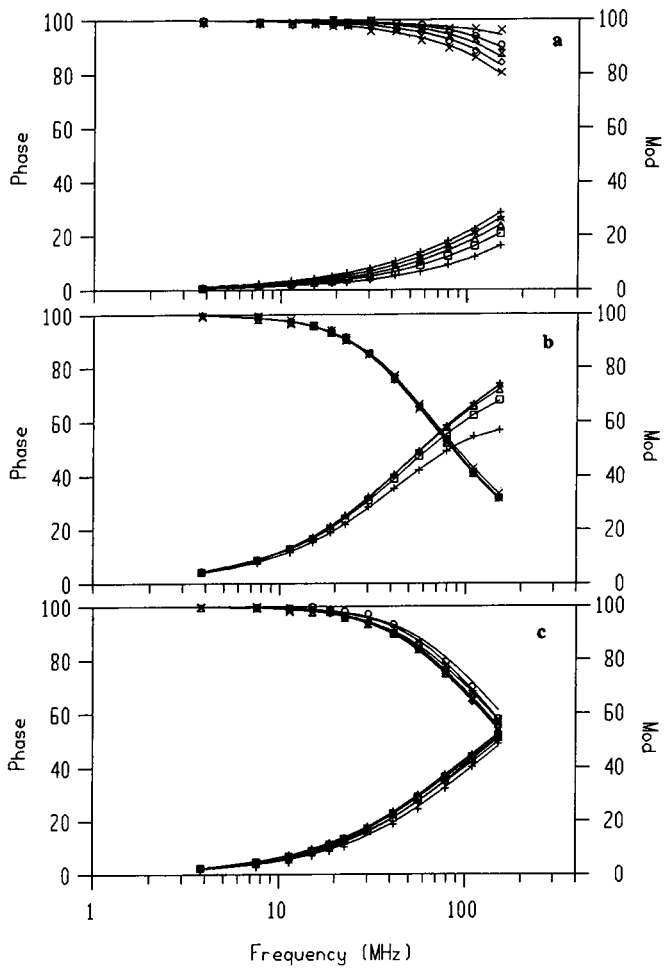

FIGURE 3 Frequency response curves of DANCA in *a*) TEA, *b*) ethanol and *c*) water. Excitation was at 355 nm. Curves represent data taken across the emission band at 390, 410, 430, 450, and 470 nm in TEA; at 440, 460, 480, 500, and 520 in ethanol; and at 494, 510, 522, 530, 550, and 570 nm in water. Curves shift to lower frequency with increasing wavelength, except in water in which they first shift slightly to higher frequency and then back to lower frequency. Lines through the data points correspond to the fits with the time-invariant DAS model.

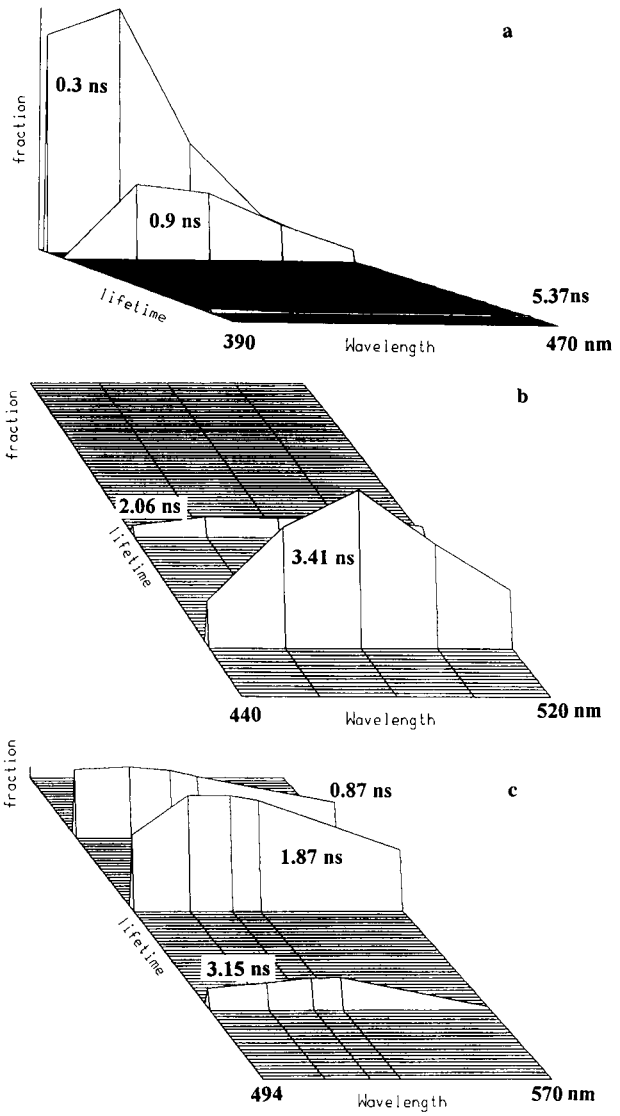

FIGURE 4 Decay Associated Spectra recovered from the analysis of the data in Fig. 5 of DANCA in *a*) TEA, *b*) ethanol, and *c*) water. DAS wavelengths are at 390, 410, 430, 450, and 470 nm in TEA; at 440, 460, 480, 500, and 520 in ethanol; and at 494, 510, 522, 530, 550, and 570 nm in water. Lifetime values for the DAS are 0.3304, 0.90, and 5.37 ns in TEA; 0.01, 2.06, and 3.41 ns in ethanol; and 0.87, 1.87, and 3.15 ns in water. The shortest DAS component in ethanol is not visible as its fractional contribution is too small to see on this plot.

time, and a second, redder component has a 0.9-ns lifetime. A very small amount of a long-lived species (5.37 ns) may not be significant. In ethanol, two DAS reasonably describe the decay, although the longer-lived, redder DAS is dominant. In water, two long-lived, red DAS (3.15 and 1.87 ns) account for two-thirds of the emission, whereas the rest is well described by a shorter-lived, blue-shifted DAS (0.87 ns).

Although the time-resolved emission heterogeneity of DANCA and similar derivatives in neat solvents and in the heme pocket of myoglobin has been interpreted in the past on the basis of dynamic relaxation (Gafni et al., 1977; Lakowicz et al., 1984; MacGregor and Weber, 1986; Bismuto et al., 1987; Bashkin et al., 1990; Pierce and Boxer, 1992), the time scales of the decay components observed here in low viscosity solvents are much too long to be explained by dynamic relaxation. The dielectric relaxation time of ethanol at 23°C is near 150 ps (Kosower, 1985; Kosower and Huppert, 1987), which is too rapid to account for the observed emission heterogeneity, whereas that of solvents such as TEA and water is even faster (Maroncelli and Fleming, 1985).

Amino derivatives of benzene and naphthalene are known to exhibit dual emission (Lippert et al., 1962, Grabowski et al., 1979, Kosower, 1985, Bashkin et al., 1990). Lippert et al. (1962) assigned the two observed bands to the ^1L_a and ^1L_b transitions, but later Grabowski et al. (1979) and Kosower (1985) (Kosower and Huppert, 1986) identified them as the locally excited (LE) and charge transfer (CT) emission transitions; Kosower has studied them in great detail (Kosower, 1985; Kosower and Huppert, 1986). Based on the model of Grabowski et al. (1979), Rollinson and Drickamer (1980) proposed that the emission of PRODAN of which DANCA is a derivative is from the LE state in apolar solvents and from the CT state in alcohols, and that the application of pressure in polar solvents results in dual emission by limiting the fraction of photons that cross-over to the CT state. These authors reported that intensity decay was homogeneous for PRODAN in all solvents, but noted that the lifetimes of the LE and CT states may have been too similar for resolution on their instrumentation. If detection is carried out at a single wavelength, as was the case in this earlier work, then emission heterogeneity is much less obvious. Clearly in TEA for example, our multi-wavelength study has brought to light considerable heterogeneity that cannot be accounted for by solvent relaxation.

We also fit the frequency response curves for DANCA in TEA to a model in which excitation was unique to the LE state (Table 1), whereas an excited-state intramolecular electron transfer reaction populates the charge transfer state. In this model proposed by Kosower (1985) absorption to the Franck-Condon level of the LE state is followed by relaxation to the lowest vibrational level of that state, in competition with conversion to the CT state. Reasonably good fits (although not as good as those to three DAS) yielded lifetimes for the two states of 0.97 and 1.2 ns, and a time constant for conversion to the charge transfer state of 500 ps. At the peak of the emission, near 400 nm, only 1–4% of the fluorescence was due to the red-emitting species. At 470 nm, this fraction reached 16%. Thus, according to this model, most of the fluorescence in TEA appears to originate from the nonpolar, LE state. The heterogeneity in ethanol and water is much less obvious than in TEA. In ethanol, only the shortest wavelength (440 nm) frequency response curve shows substantial deviation from the others (Fig. 3 *b*). There is also little heterogeneity in water, and thus we conclude that the majority of the emission in these two polar solvents, as proposed by Rollinson and Drickamer

(1980), emanates from the CT state. Bashkin et al. (1990) calculated for anilino-2-aminonaphthalene-6-dimethylsulfonamide (ANSDMA) in ethanol that the fluorescence lifetime of the LE state and the rise time for the CT state were similar, near 200 ps, whereas the fluorescence lifetime of the CT state was much longer, near 8 ns. Thus, the bulk of the emission in polar solvents was from the CT state, as we propose here for DANCA in water and ethanol.

Emission of the apoMb-DANCA complex

We now turn to the analysis of the absorption and emission properties of DANCA in the apoMb complex. The band curve fitting of the emission spectrum of DANCA in apoMb at pH 7.5 in Fig. 2c indicates heterogeneous emission from DANCA complexed in the heme pocket. The emission wavelength dependence of the frequency response curves of DANCA in apoMb (exciting primarily the LE transition at 355 nm) exhibit a very large degree of heterogeneity, with curves shifting substantially to lower frequencies with longer wavelength (Fig. 5 *a*). Such long-lived, red emission of DANCA and similar probes in apoMb has been interpreted in terms of a single time-dependent emission peak (the CT emission), that shifts red by several hundred wavenumbers over a time scale of over 25 ns (Gafni et al., 1977; Lakowicz et al., 1984; Bismuto et al., 1987; Bashkin et al., 1990; Pierce and Boxer, 1992). These authors have used these TRES to conclude that very slow relaxations of the protein matrix are responsible for the heterogeneous emission of DANCA and similar derivatives in apoMb. Although relaxation events surely occur in the heme pocket, it is not necessary that all of the observed heterogeneity arise from protein dynamics, particularly given the dual emission properties of DANCA in low viscosity neat solvents presented here.

Such wavelength dependence of the frequency response curves can also be analyzed in terms of time-invariant DAS, as we show in Fig. 6 *a*. The DAS recovered from the fit correspond to a red-shifted component at 4.2 ns and two blue-shifted components at 2.7 and 0.5 ns. In the present case we have also simulated TRES from the amplitudes and lifetimes recovered from our DAS-based fits of the data. The intensity weighted average emission energy of our simulated TRES shift from 22,340 cm^{-1} to 22,090 cm^{-1} over 25 ns. Although our TRES do not correspond exactly to those reported by previous studies (Pierce and Boxer, 1992), differences in the temperature and particularly in the pH of the samples (see below), as well as the fact that we did not acquire data over the same wavelength range as the previous studies accounts for the disparity. In any case, this exercise demonstrates that our data are equally consistent with a model of a time-dependent, red-shifting TRES, as with one assuming time-invariant DAS.

Analysis of decay data in terms of either DAS or TRES has been shown to be entirely equivalent mathematically (Beechem et al., 1985), and the red-shifting TRES does not necessarily validate the model of a single excited state undergoing time-dependent relaxation. An equally plausible explanation lies in heterogeneity in the emission, either ground or excited state. Beechem et al. (1985) noted that in the case of a DAS analysis, only the eigenvalues of the transfer matrix are recovered, and that the DAS do not represent the individual spectral components, but the inner product of the eigenvectors of the transfer matrix with the spectral contours of the emitting states. In the simple case of ground-state heterogeneity, the DAS resolve pure spectra, but in the case of an excited-state reaction they do not. A complete treatment requires analysis in terms of the species associated spectra and the rates of interconversion for the excited-state reaction. For the DANCA-apoMb system, in all probability, some complex combination of solvent relaxation and excited-state electron transfer would likely be required. In addition, the DANCA may bind to the pocket in more than one configuration, leading to ground-state heterogeneity as well. Given the heterogeneous emission in neat

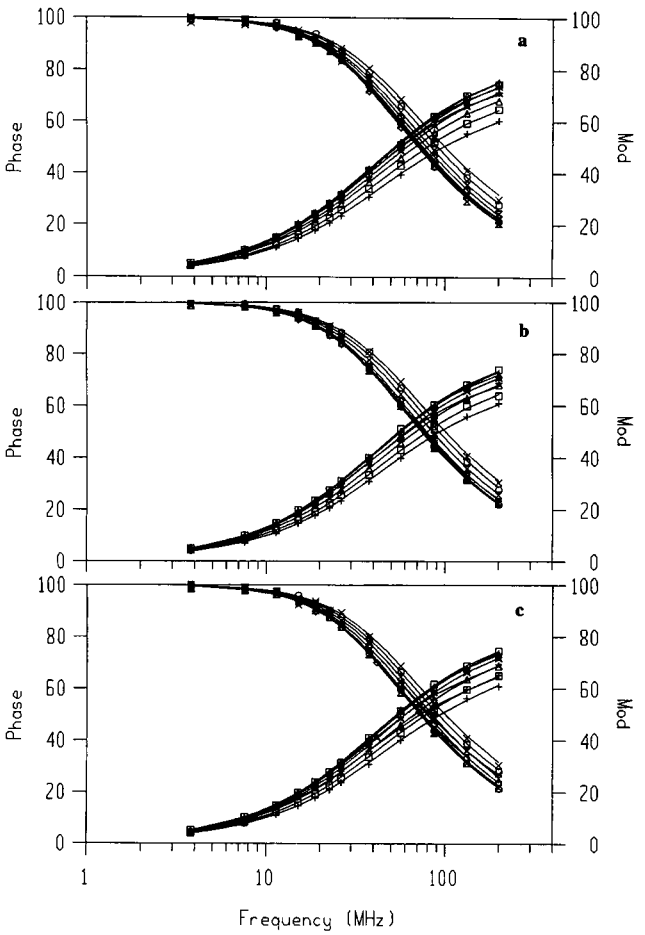

FIGURE 5 Frequency response curves for the apoMb-DANCA complex as a function of emission wavelength for *a*) pH 5.0, *b*) pH 6.25, and *c*) pH 7.5. Emission wavelengths monitored were 410, 420, 430, 440, 450, 460, 470, 480, and 490 nm, except in *b*) where there is no curve at 490 nm. Curves shift first to lower then back to higher frequency with increasing wavelength. Lines through the data points correspond to the fits with the time-invariant DAS model.

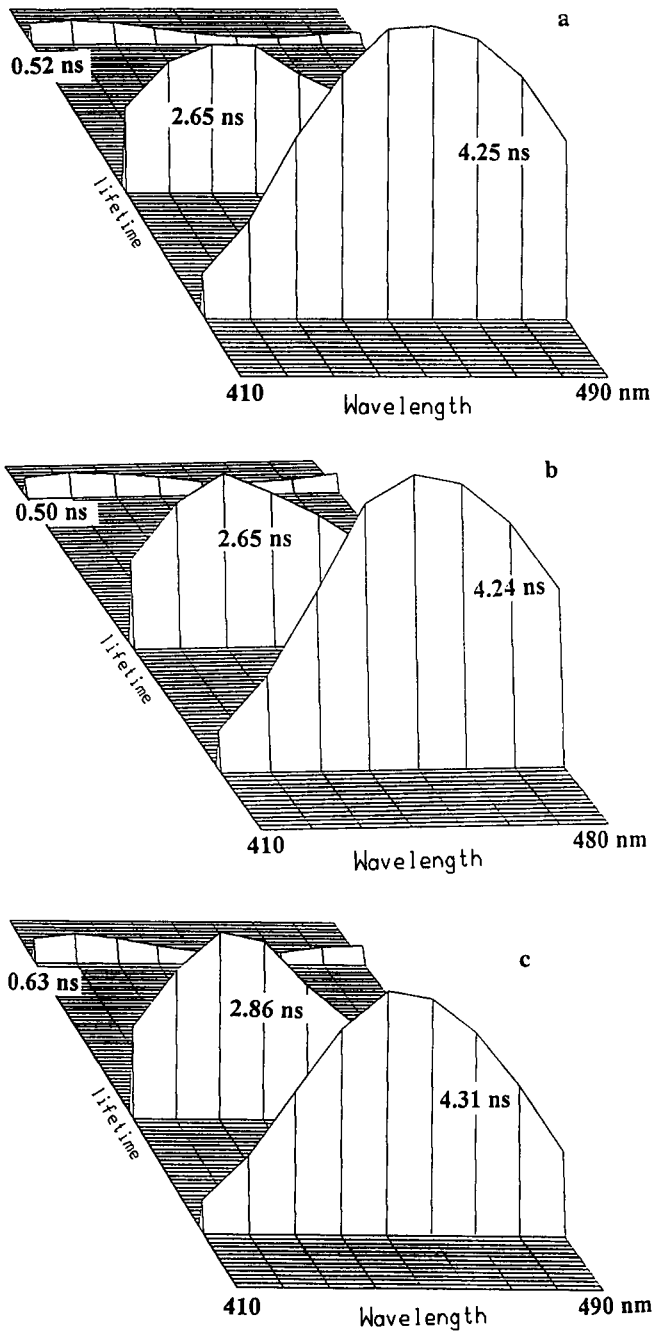

FIGURE 6 DAS for the apoMb-DANCA complex as a function of pH. *a*) pH 5.0, recovered lifetimes were 4.25, 2.65, and 0.52 ns; *b*) pH 6.25, recovered lifetimes were 4.24, 2.65, and 0.50 ns; and *c*) pH 7.5, recovered lifetimes were 4.31, 2.86, and 0.63 ns. As in Fig. 3, the wavelength range is from 410 to 490 nm in 10 nm intervals except in *b*) where there are no data at 490 nm.

solvents and the numerical equivalence of DAS and TRES analyses, we feel that it is probable that emission of DANCA in apoMb does not correspond simply to a single, time-dependent, red-shifting spectrum. Further evidence to support this notion is found in the examination of the effect of pH on the emission of apoMb-DANCA.

pH effects of the apoMb-DANCA complex

The effect of pH on the emission spectrum of DANCA bound to the apoMb heme pocket provides some insight into the photophysical origin of the DANCA emission properties in the protein complex. At the wavelength of excitation (364 nm, the maximum), direct excitation of the CT transition accounts for ~43% of the optical density. Although absorption is invariant with pH, the emission properties of DANCA are highly pH dependent. Between pH 9 and 5, the DANCA emission spectrum exhibits a decrease of ~60% of the total emission intensity, a red shift of ~400 cm^{-1} in average emission energy, and an increase of 720 cm^{-1} in the spectral bandwidth (Fig. 7). The entire spectrum does not shift; however, it is the decreased emission on the high as compared with the low energy edge that leads to the change in the average emission energy, as well as the large increase in bandwidth. Moreover, the DANCA remains bound, because the red shift is insufficient to resemble the emission of DANCA in water.

To elucidate whether or not this pH-induced decrease in emission intensity of DANCA in the heme pocket resulted from dynamic quenching, lifetime measurements were carried out at pH 6.25 and 5.0 as a function of emission wavelength (Fig. 5, *b* and *c*). Simple comparison of these frequency response curves with those obtained at pH 7.5 reveals that there is little, if any, pH effect on the decay properties. As before, analysis of the data for pH 5 and 6.25 was carried out in terms of time-invariant DAS and yielded

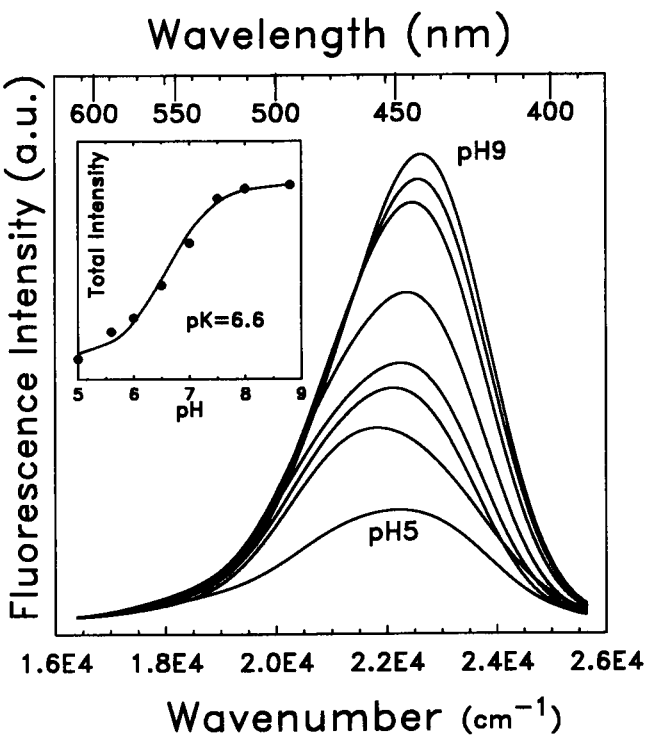

FIGURE 7 Corrected emission spectra of DANCA in apomyoglobin as a function of pH. The inset shows the evolution of the fluorescence intensity at 440 nm as a function of pH. Excitation was at 364 nm.

TABLE 3 Emission wavelength dependence of the fractional contributions of the lifetime components compared to those of the steady-state emission components at pH 5.0

λ (nm)	410	420	430	440	450	460	470	480	490
$f_{\tau 1}$ 4.25 ns	0.278	0.376	0.507	0.594	0.688	0.736	0.788	0.810	0.749
$f_{\tau 2}$ 2.65 ns	0.578	0.531	0.434	0.370	0.289	0.251	0.198	0.161	0.206
$f_{\tau 3}$ 0.52 ns	0.143	0.093	0.060	0.036	0.022	0.014	0.014	0.029	0.045

The f_τ values correspond to the fractional intensity pre-exponential factors for each of the three lifetime components.

results quite similar to those obtained at pH 7.5, a (~0.5–0.6 ns) blue lifetime, another longer (2.7 ns) blue lifetime and, finally, a third red one (4.3 ns). The parameters recovered from the global fits can be found in Tables 3–5. The recovered DAS at all three pH values can be found in Fig. 6, *a–c*. At pH 5, the long-lived reddest DAS is red-shifted with respect to its position at the higher pH values, and its contribution to the overall intensity is ~10–15% higher than at the higher pH values.

It is obvious from examination of the data, that while pH has a large effect on the steady-state emission intensity and average energy of DANCA in apoMb, there is very little change in the lifetimes. Regardless of the decay analysis scheme, the average lifetimes calculated for the blue-edge, red-edge and middle of the spectrum are the same at pH 7.5 and 5. We also note that there is no effect of pH on the emission properties of DANCA in water, and thus, the observed changes in the steady-state emission must arise as a result of complexation with the protein. The observed shift in the spectrum can be explained in terms of either dynamic relaxation, conformational heterogeneity or dual emission. In the case of dynamic relaxation, one would argue that the protonation of some nearby amino-acid residue(s), most likely the pocket histidines, could lead to an increase in the polarity of the pocket and a greater degree of relaxation. If an increase in heme pocket polarity is the cause of the red shift in emission, then one would expect to observe a red shift of the absorption spectrum as well, because of direct stabilization of the Franck-Condon state (See Fig. 1). Moreover, one would also expect that the CT absorption transition should be enhanced in a more polar environment (as is apparent in the absorption spectra in Fig. 1). Neither of these phenomena is observed. The absorption spectrum of DANCA in apoMb is pH independent. In contrast, the pH behavior of the emission spectrum is consistent with static quenching, resulting in increased contribution of the red-emitting species relative to the blue at low pH.

The pH range over which the changes in the steady-state emission properties (intensity, maximum, and bandwidth) are observed and the shape of the curve (*inset* in Fig. 7) implicate the protonation of one or more histidine residues. The pK_a obtained from the analysis of the intensity data as a function of pH is 6.6. Cocco et al. (1992) were unable to assign the resonances for the pocket histidines of apoMb, such that comparison with their results is not possible. However, because DANCA binds in the heme pocket, it is reasonable to assume that the protonation equilibrium reported upon by the quenching of the DANCA fluorophore corresponds to the titration of the pocket histidines. It is known that histidine is an effective quencher of indole fluorescence by means of complexation (Van Gilst et al., 1993). In the case of histidine quenching of DANCA, static quenching through ground-state complexation may be much more efficient when the histidines are protonated.

Pressure effects on the apoMb-DANCA complex

The effect of pressure on the fluorescence emission of free DANCA and the apoMb-DANCA complex was investigated at different pH values. Regardless of the pH, the major effect of pressure is to drastically decrease the overall fluorescence of DANCA in the heme pocket, whereas it only slightly affects that of free DANCA (Fig. 8). This drastic pressure-induced decrease of the apoMb-DANCA emission intensity is completely reversible when the pressure is released. The pressure-dependence of the frequency response curves of the apoMb-DANCA complex at pH 6.2 and up to 2.5 kbar showed very little change in the fluorescence lifetimes (data not shown), indicating that, as was the case with the pH effects, the decrease in total fluorescence intensity as a function of pressure is mainly due to a static quenching mechanism. We can rule out the effect of pressure on the solution pH as we have used a pressure independent buffer (Tris) (Neuman et al., 1973). The evolution of the fluorescence intensity at the maximal emission wavelength as a function of pressure yields an S-shaped curve (Fig. 9 *c*) with a midpoint near 1300 bar. This suggests a two-state equilibrium of the DANCA environment.

TABLE 4 Emission wavelength dependence of the fractional contributions to the lifetime components compared to those of the steady-state emission components at pH 6.25

λ (nm)	410	420	430	440	450	460	470	480
$f_{\tau 1}$ 4.24 ns	0.259	0.352	0.470	0.602	0.669	0.716	0.732	0.677
$f_{\tau 2}$ 2.65 ns	0.609	0.556	0.472	0.358	0.304	0.259	0.232	0.255
$f_{\tau 3}$ 0.50 ns	0.132	0.0092	0.059	0.040	0.027	0.025	0.036	0.067

The f_τ values correspond to the fractional intensity pre-exponential factors for each of the three lifetime components.

TABLE 5 Emission wavelength dependence of the fractional contributions of the lifetime components compared to those of the steady-state emission components at pH 7.5

λ (nm)	410	420	430	440	450	460	470	480	490
$f_{\tau 1}$ 4.31 ns	0.209	0.292	0.319	0.504	0.618	0.681	0.711	0.681	0.535
$f_{\tau 2}$ 2.86 ns	0.628	0.596	0.540	0.455	0.353	0.295	0.253	0.243	0.346
$f_{\tau 3}$ 0.63 ns	0.162	0.113	0.068	0.041	0.029	0.024	0.036	0.075	0.119

The f_τ values correspond to the fractional intensity pre-exponential factors for each of the three lifetime components.

The increased emission of free DANCA <~19,500 cm^{-1} (>510 nm) as a function of pressure (Fig. 8) suggests that some DANCA leaves the heme pocket when pressure is applied. To elucidate this point, anisotropy measurements were performed as a function of pressure with a 530-nm high pass filter to select the spectral domain where the free DANCA emits (Fig. 9 *a*). Assuming to a first approximation, that the increased intensity on the red edge of the spectrum was due entirely to an increased contribution of free DANCA, the spectrum observed at 2500 bar was subtracted for a corresponding amount of the free DANCA emission spectrum at the same pressure. This allows one to estimate at 2500 bar the fraction of free and bound DANCA and, subsequently, a K_d value of 340 μM, an order of magnitude higher than the K_d at atmospheric pressure. The normalization of the peak intensity for the decreased bound fraction shows that DANCA escape into the external solvent accounts for only 20% of the total intensity decrease upon application of pressure. At 2500 bar, 54% of the DANCA remains bound. This means that 80% of the observed pressure-induced quenching cannot be explained by DANCA expulsion, but must arise from changes in the interaction between bound DANCA and the heme pocket environment.

A pressure transition is observed both for the average emission energy and the intensity of the bound DANCA (Fig. 9, *b* and *c*), implying that the protein-DANCA complex evolves toward a conformation exhibiting a lower affinity for the DANCA rather than a continuous dissociation of the apoMb-DANCA complex or a complete unfolding of the protein. Analysis of the average emission energy and intensity profiles (Fig. 9, *b* and *c*) in terms of the free energy and volume change for this conformational transition both yield a ΔV of near −85 ml/mole and a free energy of −2.6 kcal/mole. The pH dependence of the pressure effects (data not shown) demonstrated that increasing pressure and decreasing pH resulted in similar DANCA emission properties, indicating that pH and pressure stabilize similar forms of the apoMb-DANCA complex.

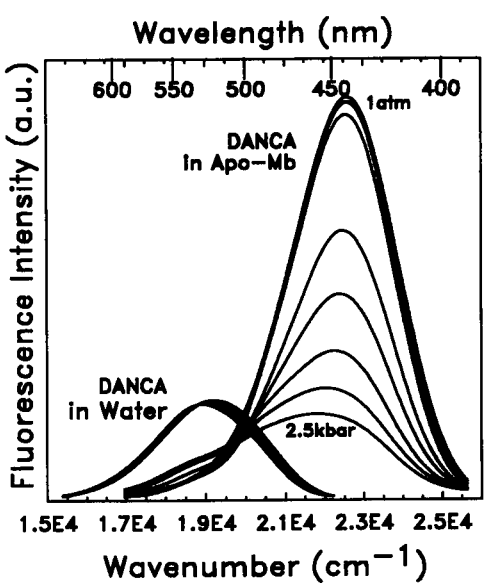

FIGURE 8 Corrected emission spectra of DANCA in apomyoglobin and water as a function of pressure. Excitation was at 364 nm.

CONCLUSIONS

The DANCA probe exhibits complex photophysical behavior that is acutely sensitive to its environment. Absorption and excitation spectra are consistent with the electronic transitions that have been demonstrated or proposed for naphthylamine type derivatives. Strong charge transfer absorption is apparent in polar solvents. Two other transitions are apparent in the excitation spectra under one broad absorption peak that may correspond to the ^1L_b and ^1L_a transitions.

Emission wavelength heterogeneity of the decay parameters of DANCA in a series of low viscosity solvents on nanosecond time scales indicates that dual emission is observed to some degree in all solvents tested, although we propose that emission from the nonpolar locally excited state is favored in the apolar solvent, TEA, and charge transfer emission dominates in polar solvents. Based on the dual emission in low viscosity solvents and the evolution of the fluorescence properties of DANCA in the apoMb heme pocket with pH, we propose that dual emission may also occur in the protein environment. Analysis of the time-resolved fluorescence of DANCA in apoMb in terms of heterogeneous decay is equally valid as analysis in terms of a single component red-shifting with time. Nonetheless, it is certain that dynamic relaxation also contributes to the fluorescence emission properties of DANCA in the heme pocket, because at very short times, rising red edge emission is observed using instrumentation with a faster time response (Pierce and Boxer, 1992). This does not mean that all of the wavelength heterogeneity of the decay need arise from relaxation phenomena. Moreover, the DANCA molecule within the heme pocket may bind in more than one

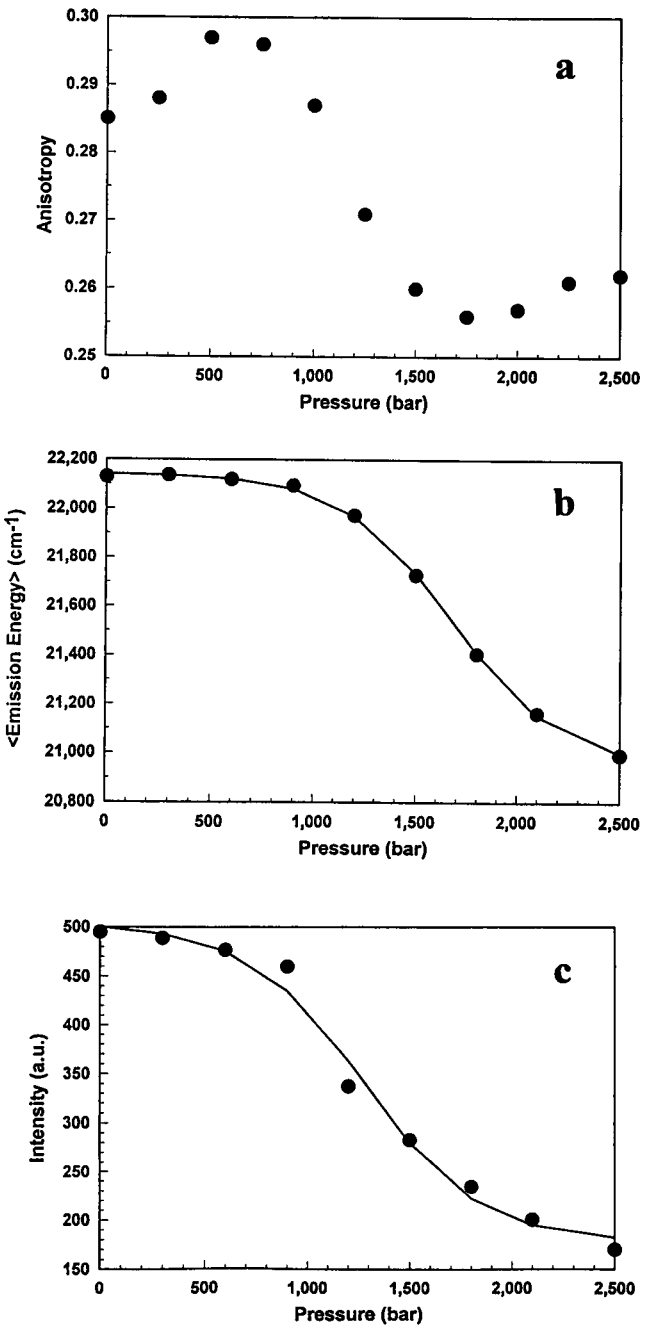

FIGURE 9 Pressure effects on DANCA fluorescence parameters. *a*) Evolution of the anisotropy, *b*) evolution of the average emission energy, and *c*) evolution of the intensity of DANCA in apoMb as a function of pressure at 20°C. The intensity data yielded a ΔG of -2.6 kcal/mol and a ΔV of -80 ml/mol, while the average emission energy yielded a ΔG of -2.7 kcal/mol and a ΔV of -85 ml/mol.

configuration, such that there may be ground-state conformational heterogeneity of the bound DANCA, as well. If DANCA in the heme pocket truly does emit from both a red-shifted charge transfer state and a blue-shifted nonpolar state, or alternately from multiple confromational states, then the analysis of DANCA decay in the pocket based on a single time-dependent peak shifting red because of dynamic relaxation of the surrounding protein matrix may tend to overestimate the time scales of these relaxation events.

The pH and pressure dependence of the absorption and emission properties of DANCA in apoMb support the model of dual emission. These data also indicate a ground-state complexation between DANCA and the pocket histidines. Pressure apparently causes a conformational change in the protein that leads to a ~12-fold decrease in affinity for the DANCA probe. That the apoprotein is completely unfolded at 2500 bar is unlikely because 50% of the DANCA exhibits the spectral properties of DANCA bound to apoMb and not those observed in water. The similarity in the effects of pH and pressure on the emission properties of the DANCA suggests that the form of the protein favored at high pressure may be similar to that favored at pH 5. This may correspond to a somewhat looser, more hydrated structure, based on the substantial negative volume change observed in the pressure studies. However, it is clearly much more structured than the well-studied acid intermediate (I) of apoMb. The pH midpoint of this intermediate is well below pH 5.0 (Goto and Fink, 1990, Barrick and Baldwin, 1993). Moreover, the free energy difference between the native state and the I state is nearly 5 kcal/mole (Barrick and Baldwin, 1993). In addition, NMR studies have indicated that the heme pocket is completely disrupted in this intermediate, which exhibits structure only in the AGH subdomain (Hughson et al., 1990). Finally, protonation of histidines 24 and 119, not the pocket residues, are implicated in the formation of the I state (Barrick et al., 1994). The fact that DANCA remains bound to a significant degree at 2500 bar indicates at least partial integrity of the heme pocket. Moreover, the stability of this state is only 2.6 kcal/mole lower than the native form. Structurally and energetically this novel conformation of apoMb appears to lie between the native and I states.

These studies were funded by a grant from the Graduate School of the University of Wisconsin to CAR. OS was funded by a grant from the French Ministry of Research. BA was partly funded by the Fondation de la Recherche Médicale. We are grateful to Professors Gregorio Weber and Harry Drickamer for helpful discussions and insights.

REFERENCES

Barrick, D., and R. L. Baldwin. 1993. Three-state analysis of sperm whale apomyoglobin folding. *Biochemistry.* 32:3790–3796.

Barrick, D., F. M. Hughson, and R. L. Baldwin. 1994. Molecular mechansims of acid denaturation: the role of histidine residues in the partial unfolding of apomyoglobin. *J. Mol. Biol.* 237:588–601.

Bashkin, J. S., G. McLenndon, S. Mukamel, and J. Marohn. 1990. Influence of medium dynamics on solvation and charge separation reactions: comparison of a simple alcohol and a protein solvent. *J. Phys. Chem.* 94:4757–4761.

Beechem, J. M., M. Ameloot, and L. Brand. 1985. Global analysis of fluorescence decay surfaces: excited state reactions. *Chem. Phys. Lett.* 120:467–471.

Beechem, J. M., E. Gratton, M. Ameloot, J. Knutson, and L. Brand. 1992. The global analysis of fluorescence intensity and anisotropy data: Second generation theory and programs. *In* Topics in Fluorescence Spec-

troscopy, Vol. 2, Principles. J. R. Lakowicz, editor. Plenum Publishing, New York. 241–305.

Bismuto, E., D. M. Jameson, and E. Gratton. 1987. Dipolar relaxation in glycerol: a dynamic fluorescence study of 4-2′-(Dimethylamino)-6′-naphthoylcyclohexanecarboxylic acid (DANCA). *J. Am. Chem. Soc.* 109:2354–2357.

Cocco, M. J., Y.-H. Kao, A. T. Phillips, and J. T. J. Lecomte. 1992. Structural comparison of apomyoglobin and metaquomyoglobin: pH titration of histidines by NMR spectroscopy. *Biochemistry.* 31: 6481–6491.

Fleming, G. 1986. Subpicosecond spectroscopy. *Ann. Rev. Phys. Chem.* 37:81–104.

Gafni, A., R. P. DeToma, R. E. Manrow, and L. Brand. 1977. Nanosecond decay studies of a fluorescence probe bound to apomyoglobin. *Biophys. J.* 17:155–168.

Goto, Y., and A. L. Fink. 1990. Phase diagram for acidic conformational states of apomyoglobin. *J. Mol. Biol.* 214:803–805.

Grabowski, Z. R., K. Rotkiewicz, A. Siemiarczuk, D. J. Cowley, and W. Baumann. 1979. Twisted intramolecular charge transfer states (TICT). A new class of excited states with full charge separation. *Nouv. J. Chim.* 3:443–454.

Hughson, F. M., P. E. Wright, and R. L. Baldwin. 1990. Structural characterization of a partly folded apomyoglobin intermediate. *Science.* 249:1544–1548.

Ilich, P., and F. G. Prendergast. 1989. Singlet adiabatic states of solvated PRODAN: a semiempirical orbital study. *J. Phys. Chem.* 93:4441–4447.

Kendrew, J. C., R. E. Dickerson, B. E. Standberg, R. G. Hart, D. R. Davies, D. C. Phillips, and V. C. Shore. 1960. Structure of myoglobin. A three dimensional Fourier synthesis at 2 Å resolution. *Nature.* 185:422–427.

Kosower, E. M. 1985. Mechanism of fast intramolecular electron transfer reactions. *J. Am. Chem. Soc.* 107:1114–1118.

Kosower, E. M., and D. Huppert. 1986. Excited state electron and proton transfers. *Ann. Rev. Phys. Chem.* 37:127–156.

Lakowicz, J. R., E. Gratton, H. Cherek, and G. Laczko. 1984. Determination of time-resolved emission spectra and anisotrpies of a fluorophore-protein complex using frequency domain phase modulation fluorometry. *J. Biol. Chem.* 259:10967–10972.

Lippert, E., W. Leuder, and H. Boss. 1962. Vol. I: Fluoreszenzspektrum und Franck-Condon Prinzip in Lösungen Aromatischen Verbindungen. *In* Advances in Molecular Spectroscopy. A. Mangin, editor. Pergamon Press, Oxford, England. 443–446.

MacGregor, R. B., and G. Weber. 1986. Estimation of the polarity of the protein interior by optical spectroscopy. *Nature.* 319:70–73.

Maroncelli, M., and G. Fleming. 1987. Picosecond solvation dynamics of coumarin 153: the importance of molecular aspects of solvation. *J. Chem. Phys.* 86:6221–6239.

Neuman, R. C., W. Kauzmann, and A. Zipp. 1973. Pressure dependence of weak acid ionization in aqueous buffers. *J. Phys. Chem.* 77:2687–2691.

Pierce, D. W., and S. G. Boxer. 1992. Dielectric relaxation in a protein matrix. *J. Phys. Chem.* 96:5560–5566.

Rollinson, A. M., and H. G. Drickamer. 1980. High pressure study of luminescence from intramolecular CT compounds. *J. Chem. Phys.* 73: 5981–5996.

Royer C. A., and J. M. Beechem. 1992. Numerical analysis of binding data: advantages, practical aspects, and implications. *Methods Enzymol.* 210: 481–505.

Royer, C. A,. W. M. Smith, and J. M. Beechem. 1992. Analysis of binding in macromolecular complexes: a generalized numerical approach. *Anal. Biochem.* 191:287–295.

Royer, C. A. 1993. Improvements in the numerical analysis of thermodynamic data from biomolecular complexes. *Anal. Biochem.* 210:91–97.

Suzuki, H. 1967. Nitrobenzene, benzoic acid, aniline and related compounds. *In* Electronic Absorption Spectra and Geometry of Organic Molecules. Academic Press, New York. 477–488.

Teale, F. W. J. 1959. Cleavage of the haem-protein link by acid methylethylketone. *Biochim. Biophys. Acta* 35:543.

Van Gilst, M., C. Tang, A. Roth, and B. Hudson. 1994. Quenching interactions and non-exponential decay: tryptophan 138 of bacteriophage lysozyme. *J. Fluorescence.* 4:203–207.

Weber, G., and F. Farris. 1979. Synthesis and spectral properties of a hydrophobic fluorescent probe: 6-propionyl-2-(dimethylamino)naphthalene. *Biochemistry.* 18:3075–3078.